

UDC 598.278:617.726

FUNCTIONAL SIGNIFICANCE OF ANATOMICAL ACCOMMODATION IN THE SKULL OF COMMON HOOPOE, *UPUPA EPOPS* (BUCEROTIFORMES, UPUPIDAE)

F. A.-R. Mahmoud¹, A. G. Gadel-Rab²

¹Department of Zoology, Faculty of Science, Assiut University, Egypt

²Department of Zoology, Faculty of Science, Al-Azhar University, Assiut, Egypt

¹Corresponding author

E-mail: M_f11_7@yahoo.com

Functional Significance of Anatomical Accommodation in the Skull of Common Hoopoe, *Upupa epops* (Bucerotiformes, Upupidae). Mahmoud, F. A.-R., Gadel-Rab, A. G. — The present study aims to supplement anatomical data about the cranial skeleton and describe some cranial modifications of the common hoopoe, *Upupa epops* Linnaeus, 1758, by using several techniques. The common hoopoe has small skull and characterized by presence of air space (pneumatization) within their bones. The degree of pneumatization increased especially within the temporal region. The skull of the common hoopoe possesses different types of kinetic hinges; one hinge locates between frontal and nasal region (frontonasal hinge) allows depression/elevation of upper beak relative to brain case. The other one exhibits between the upper beak and jugal bar (maxilla-jugal hinge). The skull of the common hoopoe characterizes by presence of powerful jaw ligamentous system. One of these ligaments exhibits ossification (Lig. Jugomandibularis medialis). In addition, a long mandibular symphysis observes between the two rami of the anterior third of the lower beak. This mandibular symphysis seems longer in the dorsal surface than the ventral one form ventral gap between the two rami of mandible. These modifications of the cranial skeleton of common hoopoe and jaw ligaments consider features of adaptation for probe mechanism, as well as exhibit its phylogenetic relationship with other avian species.

Key words: skull, pneumatization, kinetic hinge, jaw ligament, hoopoe.

Introduction

The common hoopoe is a colorful bird species which possesses some unique external features and has its own foraging style (Kristin, 2001; El-Bakary, 2011; Gadel-Rab, 2017; Mahmoud et al., 2018). Recently, the hoopoe has been the object of interest by many scientists to clarify its phylogenetic relationship between bird species. These studies led to separate the hoopoe from Coraciiformes into another order and then in 2017, it has been joined with the hornbills into Bucerotiformes order (Mayr, 2000; Gill & Donsker, 2017). Although, we were noticed that many molecular studies were concentrated on the phylogenetic relationships between bird species (Lavinia et al., 2019; Barreira et al., 2016; Lijtmaer et al., 2012; Campagna et al., 2012) but the study of avian cranio-mandibular system is still an interesting subject (Demmel Ferreira et al., 2019; Zelenkov, 2017; Fabbri et

al., 2017; Ni et al., 2017) to try understand the functional ecological classification of bird species beside clarify some modifications that specific to each species (species-specific feature).

Through the literature, we found that there are only Rawal (1968) whose gave attention to the hoopoe feeding apparatus and he is still the best illustration of hoopoe's feeding system in spite of it was depending only on gross anatomy. Thus, the main aim of the present study was to supplement anatomical data about the cranial skeleton and describe some cranial modifications of the common hoopoe by using several techniques e. g. gross anatomy; scanning electron microscopy and alizarin-red staining of bones to clarify certain individual features of the cranial skeleton of the common hoopoe as well as describe its jaw ligament system.

Material and methods

Ten specimens of the common hoopoe, *Upupa epops* (order Bucerotiformes) were obtained from Abou Rawash (North Giza, Egypt). All specimens were brought at the Assuit University in the vertebrate comparative anatomy Lab., and dissected in compliance with guidelines of the research ethics committees, Assuit University (www.enrec.org). Seven specimens were used in preparation of skull and mandible by using wild-stereomicroscope. The skull and mandible were drawing by the camera Lucida and photographed by using a digital camera. Some specimens were stained with Alizarin red according to Salaramoli et al. (2015). All measurements were taken from digital photographs using Image J software and analysis made using Excel statistical package. We followed Nomina Anatomica Avium (Baumel et al., 1993) for osteological terminology and some nomenclature modifications of hoopoe's skull and mandible.

Anatomical abbreviations: Bc, Brain case; F, Frontal; DF, Frontal depression; P, Parietal; Si, interorbital septum; L, Lacrimal; J, Jugal; Uj, Upper jaw; Q, quadrate; et, ectoethmoid; Z pr., zygomatic process; Po pr., postorbital process; Cq, quadrate body; Ns, Nasal septum; NI, Proximal nostril; NII, distal nostril; Lj, Lower jaw; Fmm, Medialis mandibulae fossa ; Flm, Lateralis mandibulae fossa; Ccm, Crista caudalis mandibularis; FQ, Quadratic articular fossa ; C pr., Coronoid processes; Art, Articular; Ra pr., Retroarticular process; Mm pr., Medial process of mandible ; Tc, Transverse crest; Cm, Medial cotyla; Cl, Lateral cotyla; Ft, Temporal fossa; Fst, Subtemporal fossa; Cn, Nasal concavity; Clq, Lateral condyle of mandibular process; Cmq, Medial condyle of mandibular process; Orq pr., Orbital process of quadrate; Jdc, Dorsal condyle of jugal; JVC, Ventral condyle of jugal; Ot pr., Otic process of quadrate; Sqc , squamosal condyle of otic process; Co, Otic condyle of otic process; Pl, Palate; M pr., Process of maxillae; Lp, Paris Lateralis; Lc, Lateral crest; Fv, Ventral Fossa; Pt, Pterygoid; Rp, rostrum parasphenoid; Brp, projection rostrum parasphenoid; Ls, lateralosphenoidale; Cls, Crista lateralosphenoidale; Bs, Basitemporal; LBs, Lateralisbasitemporalis; Bo, Basioccipital; Ex, Exoccipital; So, Supraoccipital; Fm, Foramen Magnum; Lig.Jml, Jugomandibularis lateralis ligament; Lig.Jmm, Jugomandibularis medialis ligament; Lig.Om, Occipitomandibularis ligament; Lig.Po, Postorbital ligament.

Results

The present study attempts to give more details about some regions of brain case of the common hoopoe that are relevant for the attachment of jaw ligamentous system and flexion zones.

The common hoopoe has small brain case (Bc) which is characterized by presence of great air spaces within bone elements (pneumatization).

Roof and lateral bones of brain case

In common hoopoe, the frontal region (F) is broad concave structure (fig. 1, A–C) with deep frontal depression extends toward the parietal region divides it into two lobes (fig. 2, A). The frontal region length is (~14.14 mm) represents approximately (18 %) of the length of skull that measure about (~78.6 mm), while the frontal region width is (~9.45 mm) and constitutes about (54 %) of the width of the skull that measure about (~17.16 mm) (fig. 8, 9). The frontal region articulates anteriorly with the nasal bone (N) by conspicuous frontonasal flexion zone which is well observed by SEM (fig. 5, A). Laterally, the frontal region fuses with lacrimal bone (L) through indistinct fronto-lacrimal suture (fig. 5, A). The lacrimal bone is a small oval-shaped structure connects dorsally with the frontal region and antero-laterally with the nasal septum via conspicuous naso-lacrimal suture (fig. 1, A, B; 2, A; 5, C).

The temporal region of the common hoopoe is a wide superficial lateral area possess a wide superiorfossa (Temporal fossa, Ft) (~ 6.37 mm Length and ~ 8.77 mm width) and a

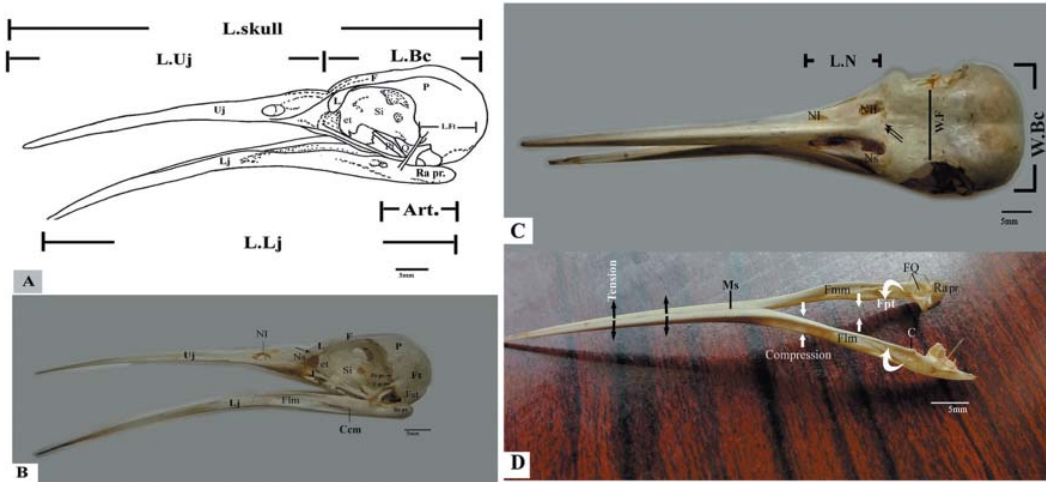


Fig. 1. A, B — lateral view, C — dorsal view of the skull and mandible of common hoopoe *Upupa epops* illustrating the bony elements and some osteometric measurements were taken in this study. In addition B, C — shows nasofrontal flexion zone (double arrows) and naso-lacrimal suture (arrow); D — photomacrograph of the dorsal surface of mandible of common hoopoe illustrate the different forces (compression and tension) resulting during contraction of pterygoideus muscle (Fpt). Scale bar 5 mm. See the list of anatomical abbreviations.

shallow sub-temporal one (Fst) (fig. 1, A, B; 2, A–C; 8; 9). The crest between the two fossae is no evident in all analyzed specimens. The superior temporal crest that fuses the temporal region dorso-laterally with the parietal region (P) is pronounced and extends anteriorly to fuse with the anterior temporal crest forming small knob (superior-temporal process, S) dorsal to the postorbital process (Po pr.) (fig. 2, A–C).

The postorbital region (Po) of the common hoopoe is a small slightly rounded process with antero-ventral orientation with length about (~1.69 mm). This process occupies about (23 %) of the length of the distance between its origin on the skull and the jugal bar (7.3 mm) with very small angle (fig. 1, B; 2, A, B; 8). Ventrally, the zygomatic process (Z pr.) which considers a prolongation of the anterior temporal crest, is well developed with tapering apex (~2.4 mm length) extends antero-ventrally to cover about (~46 %) of the quadrate body (Cq) length (~5.2 mm length) (fig. 1, B; 2 B; 8).

The upper jaw of common hoopoe (Uj) is long decurved structure (~55.18 mm length) with narrow tapering proximal apex; and broad and flat dorso-ventral base connects with the brain case. The upper jaw represents about (70 %) of the total length of the skull of the hoopoe (fig. 1, A, B; 8). Two nostrils are located dorso-laterally on the distal broad base of the upper jaw medial to the nasal septum. The proximal nostril (NI) is a small rounded-shaped aperture, while the distal nostril (NII) is long oval-shaped one (fig. 1, B, C). Slight deep nasal concavity (Cn) (~5 mm length) connects between the two nostrils and occupies about (9 %) of the length of upper jaw (fig. 9). The nasal septum (Ns) extends from the anterior nostril to articulate distally with the frontal and lacrimal bones through clearly flexion zone (fig. 5, C). The upper jaw of common hoopoe articulates postero-laterally with the jugal bar via prominent flexion zone (fig. 5, B, D).

Proximally at the articulation with the upper jaw, the jugal bar seems broad and compressed laterally. Meanwhile, at the level of the ectethmoid (et), the jugal bar (J) becomes narrow and connects with the ventral surface of the lateral process of the ectoethmoid through sheath of connective tissue (fig. 1, A, B).

The distal end of the jugal bar (J) turns to become broad and compressed at the position toward the articulation with the quadrate. Moreover, the jugal bar ends by two distal condyles; postero-dorsal condyle (Jdc) that is more elongated than the postero-ventral (Jvc) one. The two condyles of the jugal bar are articulate with the quadratojugal cotyla that

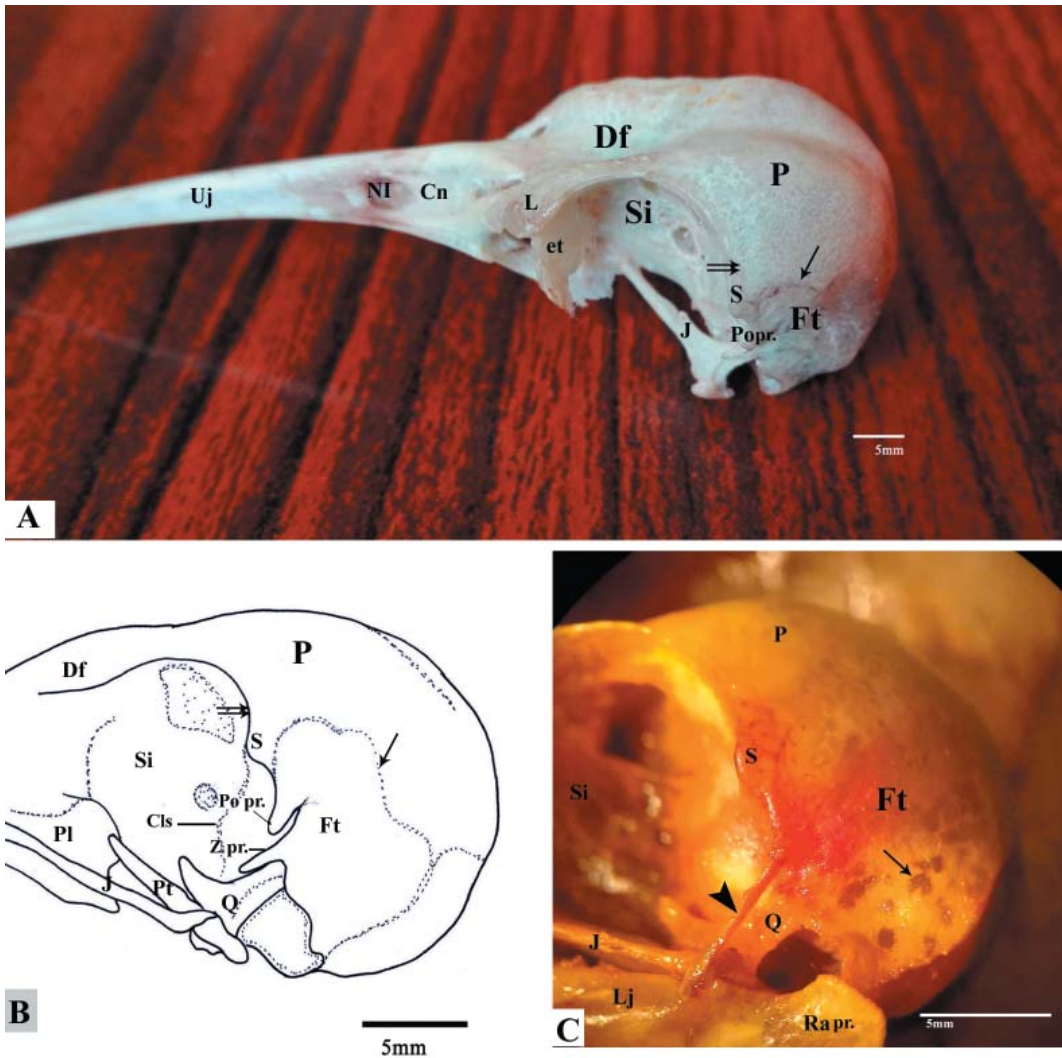


Fig. 2. Lateral view of the skull and mandible of common hoopoe *Upupa ep.*; A, B — shows the temporal region and their crests; superior temporal crest (arrow) and anterior temporal crest (double arrows); C — hotomacrophotograph of the lateral surface of skull of common hoopoe stained with Alizarin red stain showing presence of great air spaces within temporal region (pneumatization) (arrow) and postorbital ligament (arrowhead). Scale bar 5 mm. See the list of anatomical abbreviations.

is located on the lateral condyle of the mandibular process of the quadrate (Clq pr.) to form the diarthrosis articulation (Art. Quadratojugal) (fig. 1, B; 6, A, B).

The quadrate bone (Q) is triangular process articulates postero-dorsally with the brain case via two condyles of otic process (Ot pr.) and ventrally with the lower jaw via two lateral and medial condyles of mandibular process. The lateral condyle of mandibular process (Clq) orients dorso-laterally to occupy the quadratojugal cotyla. Meanwhile, small medial condyle of the mandibular process of the quadrate (Cmq) orients antero-ventrally to articulate with the pterygoid bone. The body of quadrate (Cq) extends medially to form the orbital process (Orq pr.) which has laminar shape with slightly rounded distal end (fig. 6, A–D).

Floor bones of brain case

The palate is desmognathous with broad process (Process Maxillae, M pr.) that merges with the ventral surface of maxillae and slightly expanded posteriorly to form flat plates (Pars lateralis, Lp). The pars lateralis has slight ventral curvature contains a shallow ventral

fossa (Fv) (fig. 3, A). The ventral fossa of pars lateralis exhibit faint Alizarin Red stain indicating the little degree of ossification as well as high stain appear on the lateral edges to form lateral crest of palate (Lc) (fig. 3, C). The lateral crest of palate connects tightly with the aponeurosis of *M. pterygoideus* (fig. 3, B).

Postero-medially, the palate connects with the pterygoid bone (Pt) and dorsally with the parasphenoid. The pterygoid bone is robust (6.3mm length) and represents about (26 %) of the total length of the brain case (fig. 8). The pterygoid bone articulates postero-laterally with the medial condyle of the mandibular process of the quadrate (fig. 3, A). Anteriorly, the pterygoid one possesses two articular facets; antero-medial facet connects with the postero-ventral surface of palate and dorso-medial surface of parasphenoid, and antero-lateral facet which turns dorsally to connect with the postero-dorsal surface of palate. The distal end of pterygoid has dorso-medial process (Process Muscular) just near the articulation with the quadrate (fig. 3, B).

The rostrum parasphenoid (Rp) projects ventrally forms a well-developed projection (projection of parasphenoid rostrum, Brp) (fig. 3, A). The lateralosphenoidale (Ls)

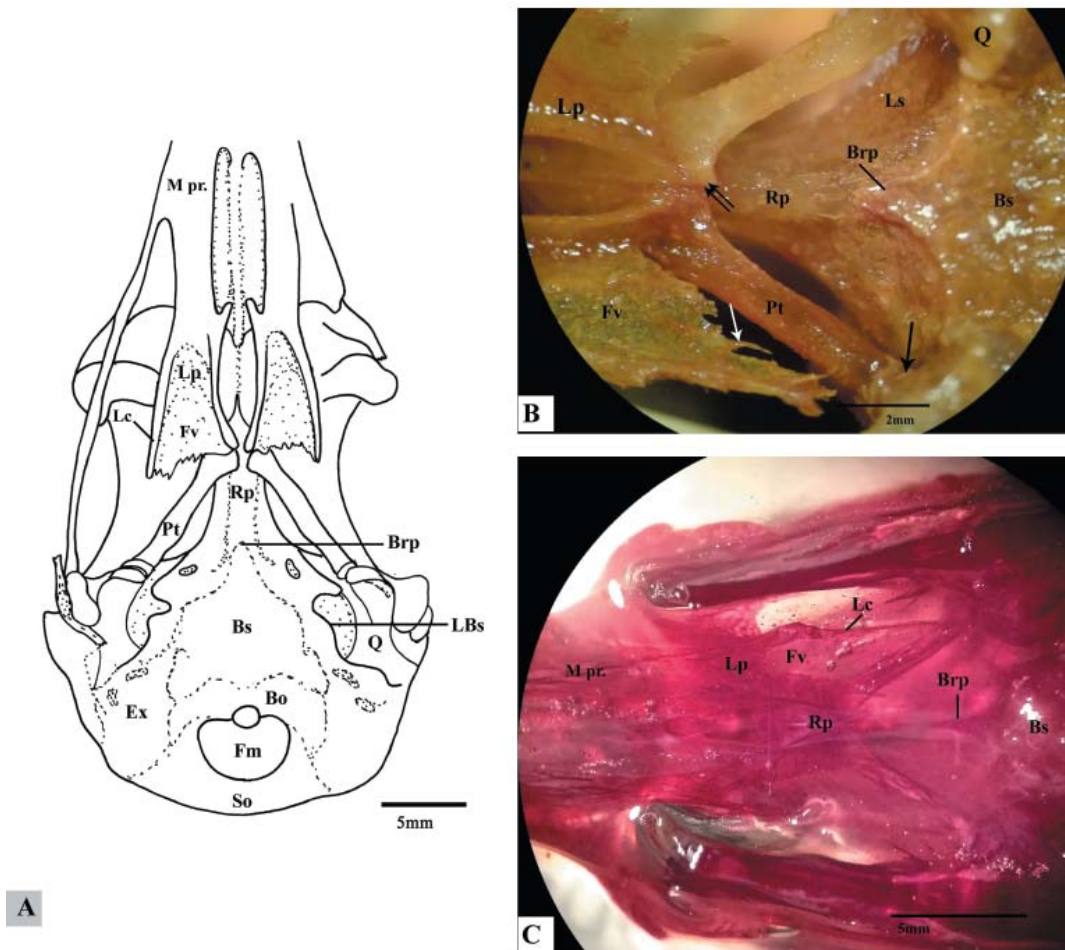


Fig. 3. Ventral view of the skull of common hoopoe *Upupa epops*: A, B — shows bony elements of floor of brain case beside reveal the articulation site between pterygoid with palate bone (double arrows) and pterygoid with quadrate (black arrow), and appearance of rudiment of aponeurosis of *M. pterygoideus* (white arrow) which connected tightly with lateral crest of palate; C — photomacrograph of the ventral surface of skull of common hoopoe stained with Alizarin red stain showing the ventral fossa of pars lateralis (Fv) gives faint red color while dense red color appear on the lateral crest of palate (Lc). Scale bar 5 mm. See the list of anatomical abbreviations.

locates posterior to orbit and connects postero-laterally with temporal region by crista laterosphenoidale (Cls) (fig 2, A, B; 3, B).

The basitemporal region (Bs) which locates postero-medially to the projection of parasphenoid rostrum possesses a well-developed lateral process (Lateralis basitemporalis, LBs) (fig. 3, A). This process connects with the medial process of the mandible through dense connective tissue.

Mandible

The lower jaw (Lj) of the common hoopoe is elongated structure with sharply pointed and decurved tip (~72.19 mm length) (fig. 1, A–D; 8). The two rami of lower jaw are fuse with each other antero-medially by mandibular symphysis (Ms) which measures about (~43.9 mm length) dorsally and (~30.30 mm length) ventrally (fig. 1, D; 9).

The intermediate portion of the mandible of hoopoe contains deep lateral fossa (lateralis mandibulae, Flm) and shallow medial one (Medialis mandibulae, Fmm) (fig. 1, B, D). Posteriorly, the lateral surface of intermediate portion of the mandible has crista caudalis mandibularis (Ccm) at the connection of the intermediate portion with the posterior portion of mandible (Articular, Art).

Moreover, the postero-dorsal edge of the intermediate portion of the mandible contains two coronoid processes (Proc. Coronoideus, C). The first process is more developed than second one and locates on the dorsal margin of the mandible, while second process situates postero-laterally to the first process (fig. 1, D).

The posterior portion of the mandible of common hoopoe (Articular, Art) measures approximately (~ 10.5 mm length), and represents about (9.5 %) of the total length of the mandible (fig. 9). The medial process (Proc. Medialis mandibularis, Mm pr.) is well developed rectangular-shaped process that orients dorso-medially, while the lateral process is absent (fig. 7, A–D). Dorsally, the posterior portion of the mandible contains deep quadratic articular fossa (FQ) (fig. 1, D) which is delimited by two cotylae; the lateral and medial cotylae. The lateral cotyla (Cl) is long and situates dorso-laterally to the fossa while the medial cotyla (Cm) is small and locates antero-dorsal to the fossa. The quadratic articular fossa bounds posteriorly by transverse crest (Tc) (fig. 7, A, C).

Posterior to the quadratic articular fossa of the mandible (FQ), projects a well-developed retroarticular process (Ra pr.) which is laterally compressed (~3.6 mm length) (fig. 7, A, C; 9). The posterior margin of the retroarticular process extends antero-ventro-medially connects with the ventral edge of the medial process of the mandible (fig. 7, B, D).

Jaw Ligamentous system

Lig. Postorbital (Lig.Po)

The postorbital ligament is a long laminar ligament extends obliquely between the distal end of the postorbital process and the postero-lateral surface of the posterior portion of the mandible just anterior to the attachment site of the Lig. Jugomandibularis lateralis (fig. 1, B; 4, A, C, D).

Lig. Jugomandibularis lateralis (Lig.Jml)

The jugomandibularis lateralis ligament is a short triangular ligament runs as broad base from the postero-lateral surface of the mandible to the dorso-lateral surface of the distal end of the jugal bar. The Lig. Jugomandibularis lateralis locates just posterior to the attachment site of postorbital ligament on the posterior portion of the mandible (fig. 4, A, D).

Lig. Jugomandibularis medialis (Lig.Jmm)

The jugomandibularis medialis ligament locates medial to Lig. Jugomandibularis lateralis and attaches on the ventral condyle of the distal end of the jugal bar. That ligament extends posteriorly around the lateral condyle of the mandibular process of quadrate to attaches on the postero-dorsal edge of the posterior portion of the mandible (fig. 4, A).

Alizarin-Red stain of the skull reveals presence of one sesamoid bone within the Lig. Jugomandibularis medialis. This sesamoid bone houses in a shallow groove which locates on the lateral condyle of the mandibular process of the quadrate (fig. 4, D). Other sesamoid bones are observed within the tendon of adductor muscle (fig. 4, C)

Lig. Occipitomandibularis (Lig.Om)

The occipitomandibularis ligament is thick ligament extends from the lateral edge of exoccipital process (Ex) to the posterior surface of the medial process of the posterior portion of the mandible (fig. 4, B).

Discussion

The present study represents the first detailed cranial osteological description for the common hoopoe. Rawal (1968) given brief information about skull of common hoopoe, he was depended only on gross anatomy in his study. He provided this information just to help in understanding the feeding mechanism of hoopoe.

The present study will exhibit more anatomical details about the cranial modifications of common hoopoe by using several techniques; gross anatomy, scanning electron microscopy

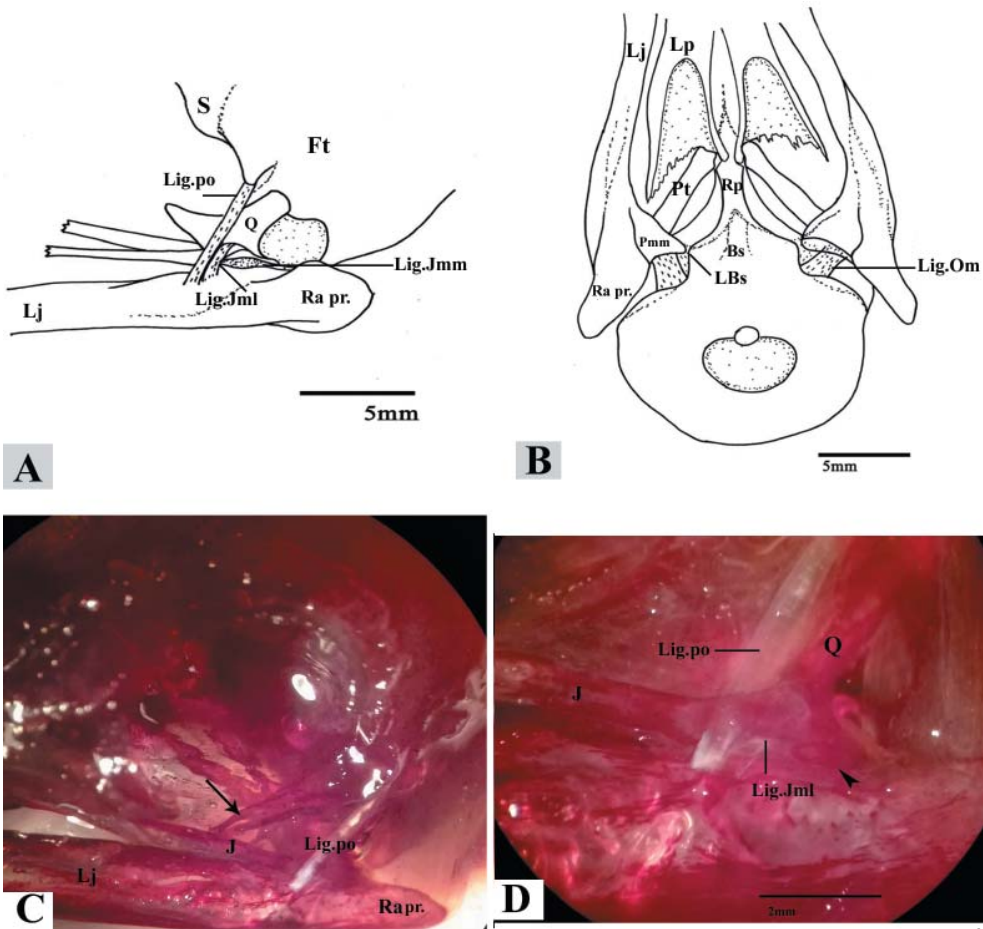


Fig. 4. Ventral view of the skull of common hoopoe *Upupa epops*: A, B — shows location of the jaw ligamentous system; C, D — photomicrograph of the lateral surface of skull and mandible of common hoopoe stained with Alizarin red stain showing small oval sesamoid bone (arrowhead) appears within Lig. Jugomandibularis medialis (Lig. Jml) and other sesamoid bones are observed within the tendon of adductor muscle (arrow). Scale bar 5 mm. See the list of anatomical abbreviations.

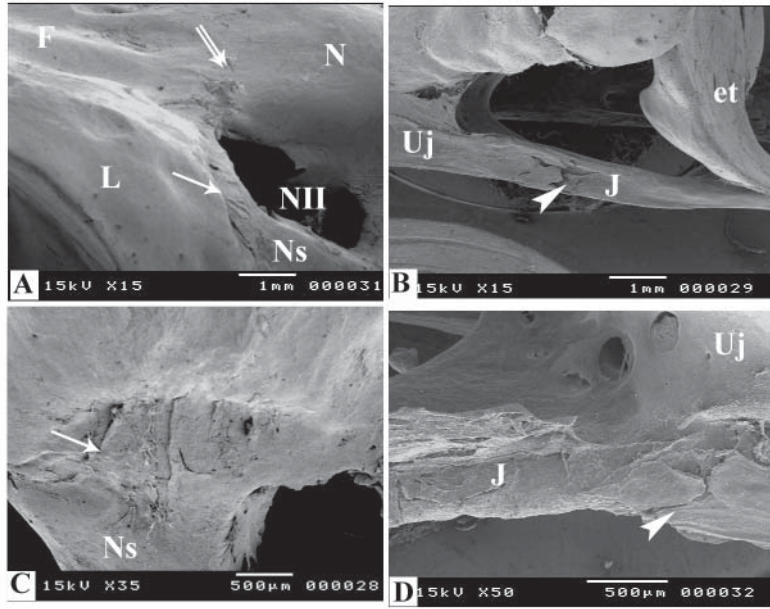


Fig. 5. Scanning electromicrograph of the skull of common hoopoe *Upupa epops* showing different positions of flexion zones between bony elements of brain case and upper jaw; Nasofrontal zone (double arrows), nasolacrimal zone (arrow) and third flexion zone (arrow head) which appears between the upper jaw (Uj) and Jugal bar (J). Scale bar 1 mm, 500 mm. See the list of anatomical abbreviations.

and alizarin-red techniques, as well as, make some morphometric measurements of the cranial skeleton of common hoopoe to reflect their individual features.

The hoopoe possess small skull which is characterized by presence of air space (pneumatization) within their bones. The degree of pneumatization increased especially

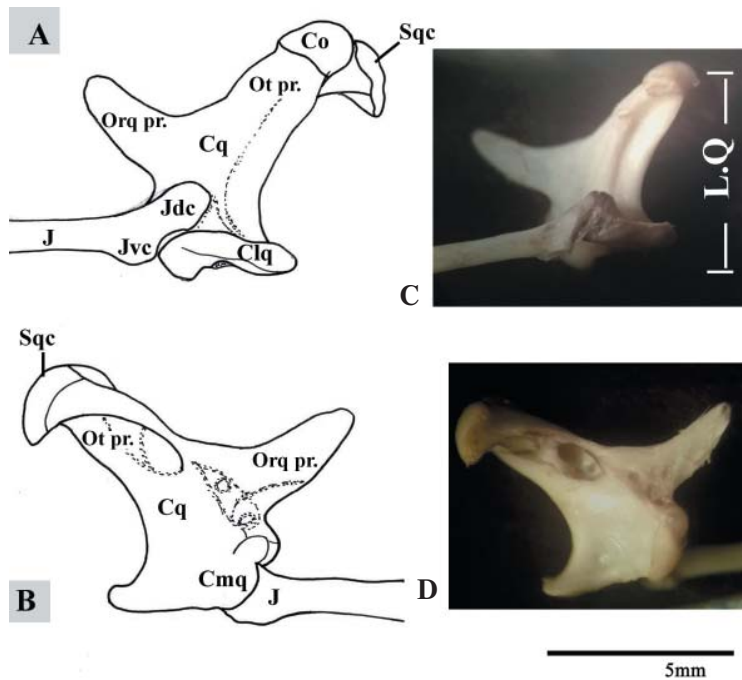


Fig. 6. Quadrate of common hoopoe *Upupa epops* (A, C — lateral view; B, D —medial view) illustrating their processes. Scale bar 5 mm. See the list of anatomical abbreviation.

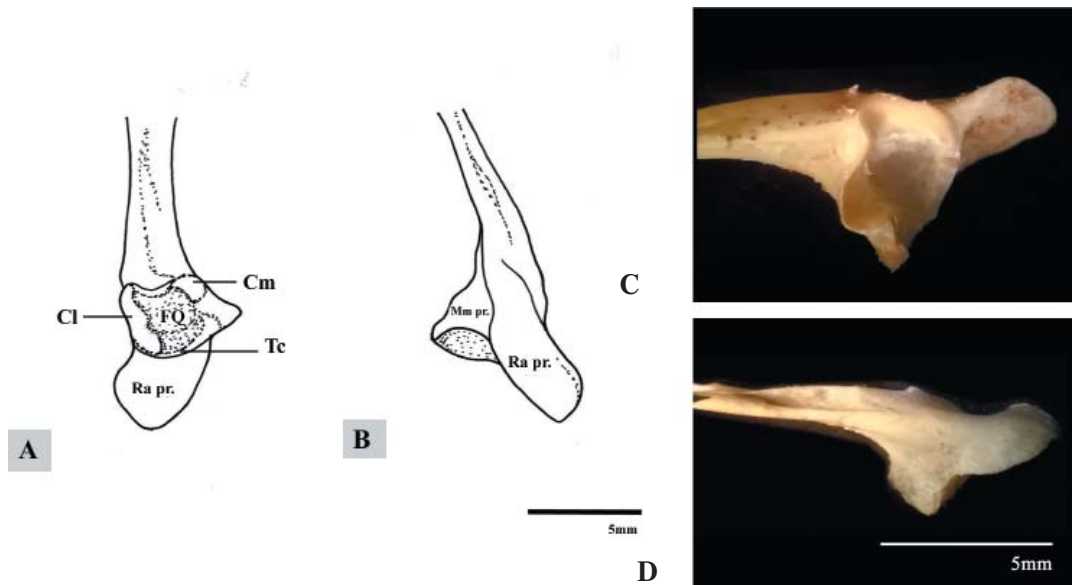


Fig. 7. Posterior portion of the mandible of common hoopoe *Upupa epops* (A, C — dorsal view, B, D — ventral view) illustrating the shape of their cotylae and processes. Scale bar 5 mm. See the list of anatomical abbreviation.

within the temporal region. The presence of pneumatization is not common in vertebrate's skulls but there are some exceptions were exhibited in crocodylians, birds and mammals (Apostolaki et al., 2015; Petritsch et al., 2011). The skeletal pneumatization assumes to be an adaptation for reducing mass and improving flight performance (Benson et al., 2012; Dumont, 2010; Harshman et al., 2008). Some previous studies had been considered that the degree of pneumatization has been a valuable tool for determine a bird's age (McKinney, 2004; Serventy et al., 1967). In fact, the exact function of skeletal pneumaticity is still not definitively known but there are several researches try to explain these hypotheses concerning the role of pneumaticity in an organism.

The authors of the present study suggest that the cranial pneumaticity may share in hearing process. The pneumaticity diverticula may collect and amplify the sound frequencies from its surrounding field like a trumpet, thereby the sound waves travel through air space cause vibration in its columella which transfers into cochlea as electrical signals. Consequently, that increases the hearing efficiency for this bird to found their prey on or under leaves and ground.

Moreover, the skull of hoopoe possesses different types of kinetic hinges; one of hinge appears between the frontal and nasal region that allows the movement of upper beak relative to brain case. Other kinetic hinge observes between the upper beak and jugal bar (maxilla-jugal hinge). These different types of kinetic hinges are common among avian species but with different degrees, e.g. in prey-predator bird like common kestrel, and black kite no any kinetic hinges between cranial elements were observed (Mahmoud et al., 2017; Shawki, 1998) while some birds like parrot possess highly movable hinge between the upper beak and brain case (Frontonasal hinge) (Mahmoud et al., 2018).

However, when testing the movement of upper beak of hoopoe against brain case, are noticed that the abduction (depress) angle of upper beak is limited or small.

The present authors are proposed two hypotheses about the role of frontonasal and maxilla-jugal hinges in common hoopoe; one of these hypotheses is that the cranial kinetic hinges permit the upper beak closes fast with the lower beak to prevent prey from escaping. The second hypothesis is that these hinges may protect the beak from twisting action during cutting prey.

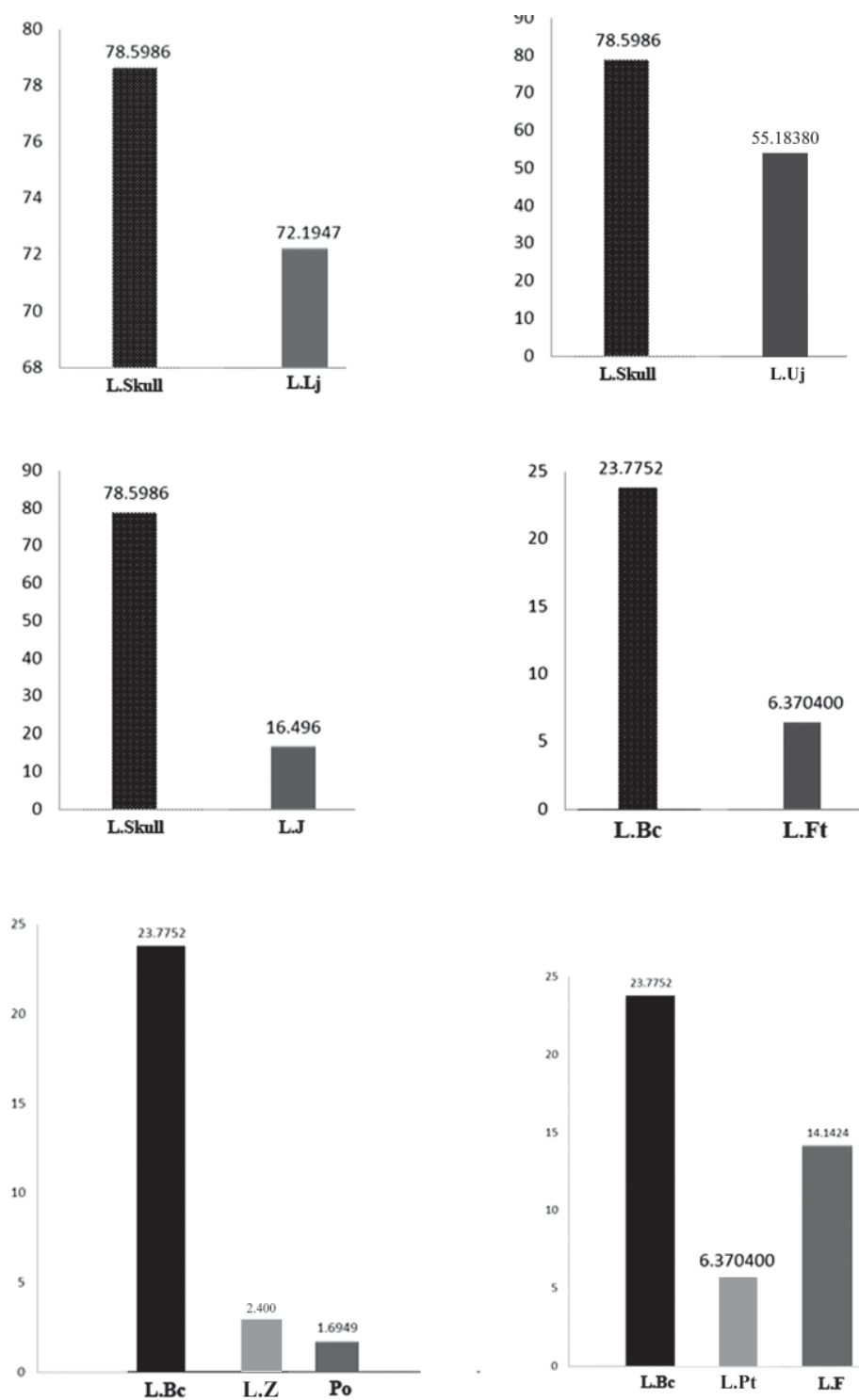


Fig. 8. Cranial osteometric characters of common hoopoe *Upupa epops* illustrate the ratio between the total length of skull, brain case and other bony elements of studied species. Abbreviations: L.skull, Length of Skull; L.Lj, Length of Lower Jaw; L.Uj, Length of Upper Jaw; L.J, Length of Jugal Bar; L.Bc, Length of Brain Case; L.Ft, Length of temporal Fossa; L.Z, Length of Zygomatic Process; Po, Length of Postorbital Process; L.Pt, Length of Pterygoid; L.F, Length of Frontal. Means in mm, N = 10.

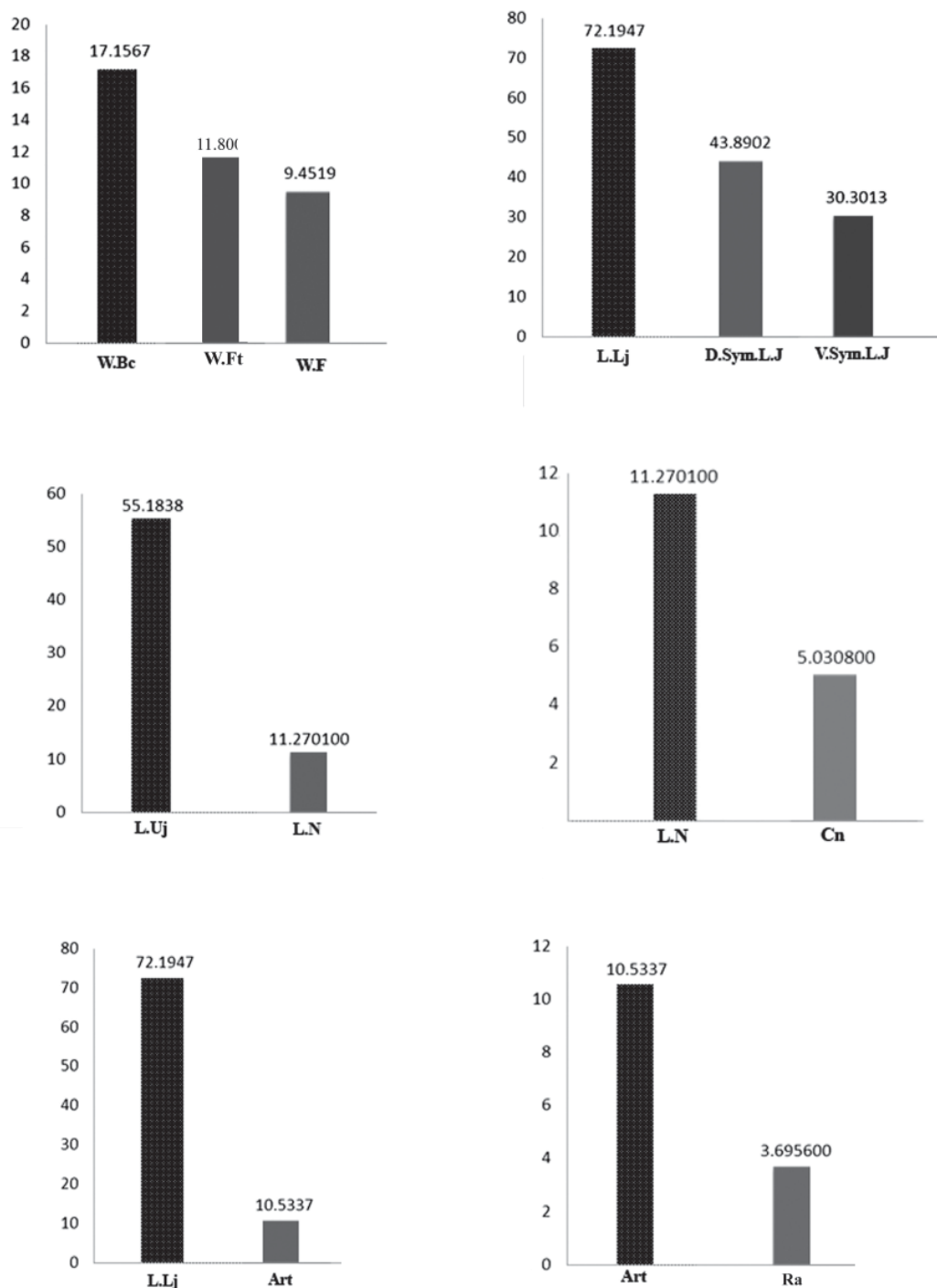


Fig. 9. Cranial osteometric characters of common hoopoe *Upupa epops*; (A) illustrate the ratio of width of brain case, temporal fossa and Frontal region; (B, E, F) illustrate the ratio between the bony elements of lower jaw and its mandibular symphysis; (c, d) illustrate the ratio between the bony elements of upper jaw. Abbreviations: W.Bc, Width of Brain Case; W.Ft, Width of Temporal Fossa; W.F, Width of Frontal; L.Lj, Length of Lower Jaw; D.Sym.L.J, Dorsal Mandibular Symphysis; V.Sym.L.J, Ventral Mandibular Symphysis; L.Uj, Length of Upper Jaw; L.N, Length of Nasal Bone; Cn, Length of Nasal Cavity; Art, Length of Articular; RA, length of Rearticular process. Means in mm, N = 10.

Obviously, the hoopoes' beaks are exposed to different forces during feeding process. Hoopoe hits their beak repeatedly on ground to cut their prey or to probe the ground. Thus, the probability of dislocation of the lower beak is expected but not occurs.

In common hoopoe, the posterior portion of lower jaw (articular) is surrounded by powerful jaw ligamentous system; Lig. Jugomandibularis lateralis, Lig. Jugomandibularis medialis and Lig. Occipitomandibularis. Furthermore, one of these ligaments provides with sesamoid bone (Lig. Jugomandibularis medialis). The present authors viewed that the presence of these powerful jaw ligamentous system around this joint beside appearance of ossification within them prevents the occurrence of dislocation phenomenon for lower beak of common hoopoe.

Moreover, the anatomical investigation of the skull of hoopoe observes that this ossification occurs not only in ligament but also appear within tendon of adductor muscle. The tendon or ligament ossification is rare in the feeding system of birds but common only in tendons of legs of vertebrates (Roeder et al., 2012; Agabalyan et al., 2013). They had proposes several adaptive explanations such as keep the position of digits or protect the tarso-metatarsus against fracture. the present authors expected that the appearance of tendon or ligament ossification within feeding system of hoopoe may has the same mechanical properties like tendons of legs in making a rigid joint that increases the effectiveness of the lower beak and avoid it from the fracture when loading heavy substance of food or stones.

However, the anatomical investigation of the brain case of the hoopoe exhibits another interesting features such as the elongated lower beak of hoopoe are fused by long symphysis. This symphysis occupies about one third of total mandible length, furthermore, the symphysis on the dorsal surface of lower jaw is longer than the ventral one that resulting in formation of ventral gap between two rami of mandible. Such long symphysis is unusual in bird species. Witmer and Rose (1991) pointed that there has been very little attention to functional analysis of the diversity of symphyseal morphology in birds and said that the symphysis between the mandibles may evolve to improve force transmission from one side to other. So, the symphysis morphology reflects attempts to buttress it against the stresses encountered during use the massive feeding system.

The mandibular rami of hoopoe are exposed to stress during contraction of pterygoideus musculature that attaches on the palatine bone and inserts on the posterior portion of mandibular rami. The contraction of this muscle tends relatively to bend the posterior half of the mandible toward ventromedial direction. Such bending causes tension along the antero-dorsal surface of symphysis and compression along its ventral surface. The long mandible symphysis in hoopoe is important in responding to bending stresses, also countering to dorsoventral shear force. Moreover, the presence of the ventral gap between the mandibular rami of hoopoe might increase the resistance of mandible to this compressive force resulting of contraction force of some muscles attached on the lower jaw.

Conclusion

Obviously, the present investigation revealed presence of some unique cranial features in common hoopoe. One of these features is the appearance of the deep depression within the frontal region. Moreover, the pneumatization within the bone of skull especially in the temporal region, as well as, the appearance of much more sites of kinetic between some bony regions of the skull. In the present study, the phenomenon of the ossification of the jaw ligaments were noted within only one of the ligament of the common hoopoe which considered as one of the features common in the hornbills bird, which plays an important role in increasing efficiency of their beaks during their feeding process. The present authors had concluded that these morphological features of the skull are considered as a hoopoe-specific trait and are closely related to the external features of this bird and their feeding style. But from the viewed of the present authors, some of these structural modifications

still need further studies to clarify the role of them in the feeding mechanism and to confirm its phylogenetic relationship between the avian species.

I would like to express our thanks to the comparative anatomy of vertebrate Lab. in Zoology Dept., Faculty of Science and electron microscopical unit, Assiut University, for their help in specimen preparations.

References

- Agabalyan, N. A., Evans, D. J. R., Stanley, R. L. 2013. Investigating tendon mineralization in the avian hind limb: a model for tendon ageing, injury and disease. *Journal of Anatomy*, **223**, 262–277.
- Apostolaki, N. E., Rayfield, E. J., Barrett, P. M. 2015. Osteological and soft tissue evidence for pneumatization in the cervical column of the ostrich (*Struthio camelus*) and observations on the vertebral columns of non-volant, semi-volant and semi-aquatic birds. *PLoS ONE*, **10** (12): e0143834.
- Barreira, A. S., Lijtmaer, D. A., Tubaro, P. L. 2016. The multiple applications of DNA barcodes in avian evolutionary studies. *Genome*, **59** (11), 899–911.
- Baumel, J. J., King, A. S., Breazile, J. E., Evans, H. E., Vanden Berge, J. C. 1993. *Handbook of avian anatomy: Nomina Anatomica Avium*. Second edition. Cambridge, MA: Nuttall Ornithological Club, 1–779.
- Benson, R. B. J., Butler, R. J., Carrano, M. T., O'Connor, P. M. 2012. Air-filled postcranial bones in theropod dinosaurs: physiological implications and the 'reptile' – bird transition. *Biol Rev*, **87**:168–193.
- Campagna, L., Benites, P., Lougheed, S. C., Lijtmaer, D. A., Di Giacomo, A. S., Eaton, M. D., Tubaro, P. L. 2012. Rapid phenotypic evolution during incipient speciation in a continental avian radiation. *Proc Biol Sci*, **7**, 279 (1734), 1847–1856.
- Demmel Ferreira, M. M., Tambussi, C. P., Degrange, F. J., Pestoni, S., Tirao, G. A. 2019. The cranio-mandibular complex of the nightjar *Systellura longirostris* (Aves, Caprimulgiformes): functional relationship between osteology, myology and feeding. *Zoology (Jena)*, **132**, 6–16.
- Dumont, R. E. 2010. Bone density and the light weight skeletons of birds. *Proc Biol Sci*. **277** (1691), 2193–8. doi: 10.1098/rspb.2010.0117
- El-Bakary, N. E. R. 2011. Surface Morphology of the tongue of the Hoopoe (*Upupa epops*). *Journal of American Science*, **7** (1), 394–399.
- Gadel-Rab, A. G., Shawki, N. A., Saber, S. A. A. 2017. Morpho-Functional adaptations of the lingual epithelium of two bird species which have different feeding habits. *The Egyptian journal of Hospital Medicine*, **69** (3), 2115–2127.
- Gill, F., Donsker, D. 2017. Todies, motmots, bee-eaters, hoopoes, wood hoopoes & hornbills. *IOC World Bird List* 7:1.
- Fabrizi, M., Mongiardino, K. N., Pritchard, A. C., Hanson, M., Hoffman, E., Bever, G. S. et al. 2017. The skull roof tracks the brain during the evolution and development of reptiles including birds. *Nat Ecol Evol*, **110**, 1543–1550.
- Harshman, J., Braun, E. L., Braun, M. J., Huddleston, C. J., Bowie, R. C. K. 2008. Phylogenomic evidence for multiple losses of flight in ratite birds. *PNAS*, **105**, 13462–13467.
- Kristin, A. 2001. Family Upupidae (Hoopoes). In: Josepedel, H., Andrew, E., Sargatal, J., eds. *Handbook of the Birds of the World*. Vol. 6, Mouse birds to Hornbills. Lynx Edicions, Barcelona, 396–411.
- Lavinia, P. D., Barreira, A. S., Campagna, L., Tubaro, P. L., Lijtmaer, D. A. 2019. Contrasting evolutionary histories in Neotropical birds: divergence across an environmental barrier in South America. *Mol Ecol*, **28** (7), 1730–1747. doi: 10.1111/mec.15018.
- Lijtmaer, D. A., Kerr, K. C., Stoeckle, M. Y., Tubaro, P. L. 2012. DNA barcoding birds: from field collection to data analysis. *Methods Mol Biol*, **858**, 127–152.
- Mahmoud, F. A., Shawki, N. A., Abdeen, A. M. 2017. Biomechanics Analysis of Jaw Musculature of the common Kestrel (*Falco tinnunculus*) and the Budgerigar (*Melopsittacus undulates*). *Bio Bulletin*, **3** (1), 39–55.
- Mahmoud, F. A., Gadel-Rab, A. G., Shawki, N. A. 2018. Functional-morphological study of the choana in different bird species. *The journal of basic and applied science*, **79**, 11.
- Mayr, G. 2000. Tiny Hoopoe-Like Birds from the Middle Eocene of Messel (Germany). *Auk*, **117** (4), 964–970.
- McKinney, R. G. 2004. Skull Pneumatization in passerines: a table of last dates many passerines in northeast can be aged safely by skulling. *North American Bird Bander*, **29** (4), 164–170.
- Ni, Y., Wang, L., Liu, X., Zhang, H., Lin, C. Y., Fan, Y. 2017. Micro-mechanical properties of different sites on woodpecker's skull. *Comput Methods Biomech Biomed Engin*, **20** (14), 1483–1493.
- Petrtsch, B., Goltz, J. P., Hahn, D., Wendel, F. 2011. Extensive craniocervical bone pneumatization. *Diagn Interv Radiol*, **17**, 308–310.
- Rawal, U. M. 1968. Anatomy of the feeding apparatus of hoopoe *Upupa epops* Linnaeus. *Proceedings of the Indian Academy of Sciences, Section B*, **68** (2), 79–90.
- Roeder, R. K., Schwartz, A. G., Pasteris, J. D. 2012. Mineral distributions at the developing tendon enthesis. *PLoS ONE*, **7**: e48630. doi: 10.1371.

- Salaramoli, J., Sadeghi, F., Gilanpour, H., Azarnia, M., Aliesfehni, T. 2015. Modified double skeletal staining protocols with Alizarin red and Alcian blue in laboratory animals. *J. J. J. J. J.*, **13**, 76–81.
- Serventy, D. L., Nicholls, C. A., Farner, D. S. 1967. Pneumatization of the cranium of the Zebra Finch *Castanotis*. *International Journal of Avian Science*, <https://doi.org/10.1111/j.1474-919X.1967.tb00026.x>
- Shawki, N. A. 1998. Kinetics of jaw apparatus of the Egyptian black Kite, *Milvus migrans aegyptius*. *J. Union. Arab. Biol. Cairo*, **9** (A), 214–255.
- Witmer, L. M., Rose, K. D. 1991. Biomechanics of the jaw apparatus of the gigantic Eocene bird *Diatryma*: implications for diet and mode of life. *Paleobiology*, **17** (2), 95–120.
- Zelenkov, N. V. 2017. Finds of fragmentary bird skeletons in the Middle Miocene of the northern Caucasus. *Dokl Biol Sci*, **477** (1), 223–226.

Received 27 September 2019

Accepted 17 October 2019